ENGINEERING TRANSACTIONS • *Engng. Trans.* • **64**, 2, 241–252, 2016
Polish Academy of Sciences • Institute of Fundamental Technological Research (IPPT PAN)
National Engineering School of Metz (ENIM) • Poznan University of Technology

Mechanical and Metallurgical Characterization of Dissimilar Weld Joints Using Continuous Direct Drive Friction Welding

Sathish RENGARAJAN[1)], Vaddi Seshagiri RAO[2)]

[1)] *Research Scholar, SCSVMV University*
Enathur, Kanchipuram, Tamil Nadu, India
e-mail: sai27r123@gmail.com

[2)] *Principal & Professor, Department of Mechanical Engineering*
St. Joseph's College of Engineering
OMR, Chennai, India

This paper presents studies on continuous direct drive friction welded joints made of low and medium carbon steels. The fractured specimen was examined using a scanning electron microscope and it consisted of fine dimples which showed the mode of ductile fracture. Plasticity which is indicative of the flow of grains was better observed in the low carbon steel side than in the medium carbon steel side. Light microscopy revealed the flow of fine grained austenite partially transformed into a marten-site structure which exhibits more tensile strength. X-ray diffraction test confirmed that the chromium in the weldments is consistently spread and improves corrosion resistance properties.

Key words: dissimilar metals, martensite ductile fracture, light microscopy.

1. Introduction

Continuous direct drive friction welding (CDDFW) is one of the solid-state joining processes in which metals are joined before the melting state. The absence of melting from the weld zone eschews oxidation, residual stress and solidification related defects in the weld joints [1]. The current trends show that dissimilar weld joints are more challenging because they have different thermal and physical properties [11]. The process parameters such as friction time, friction pressure, forging time, forging pressure, and rotation speed are the most interesting ones in the friction welding method [15]. Austenitic stainless steel X2CrNiMo17-12-2 is usually preferred to other austenitic varieties as a structural material due to its higher corrosion resistance and superior mechanical properties both at low and high temperatures [1]. In order to support the applications that demand corrosion resistance, low and medium carbon steels are

preferred. These materials with a considerable content of chromium and niobium are used as shaft, pump and nozzles in marine outboard engines [2]. Several works were conducted on friction welding on mild steel and stainless steel [8, 10]. The weld joint properties were varied by Taguchi's L9 orthogonal array to minimize the number of trials [4]. The present study investigates the joint properties such as hardness and tensile strength. The mechanical characterizations were performed according to American Society for Testing and Materials (ASTM) standards. Potentiodynamic polarization test was conducted in a 3.5 wt. % NaCl solution. X-ray diffraction (XRD) tests were carried out to study the behavior of dissimilar weld joints based on the crystallographic orientation.

2. Experimental procedure

2.1. Materials and methods

Base metals were prepared in a cylindrical form having the diameter of 23 mm and length of 75 mm. The turning process of these metals was carried out on a special purpose lathe. Before machining the surfaces of the specimens were cleaned with acetone to remove foreign materials. Their chemical compositions are shown in Table 1. The ranges of welding parameters were established and their selection is shown in Table 2. The CDDFW machine used in our study is shown in Fig. 1. To fabricate a joint using this machine, one of the two components is held stationary while the other is rotated at a certain speed. These two components are brought together so that friction takes place between the two materials; after that axial pressure (i.e., upset pressure) is given for a certain length called burn-off length.

Table 1. Chemical composition of base metals (wt. %).

Base metals/Elements	C	Mn	Si	Cr	Ni	Mo	P	S	Fe
X2CrNiMo17-12-2	0.03	2.0	0.75	17.0	10	2.0	0.03	0.01	Bal
C40	0.41	0.8	0.28	0.4	–	0.1	0.04	0.04	Bal

Table 2. Selection of welding parameters.

Parameter	Friction pressure [MPa]	Upset pressure [MPa]	Speed of rotation [RPM]	Burn-off length [mm]
Level 1	4	5	1000	3
Level 2	5	5.5	1500	4
Level 3	6	6	2000	5

FIG. 1. Friction welding machine.

3. Results and discussion

3.1. Microstructure of base metals

The microstructure of X2CrNiMo17-12-2 is shown in Fig. 2a. The presence of grain orientation indicates that the material has been roll formed. The matrix shows mixed equi-axed grains of austenite with ferrite-like microstructure; the same was reported by Kožuh *et al.* [13]. The absence of carbide parti-

a) b)

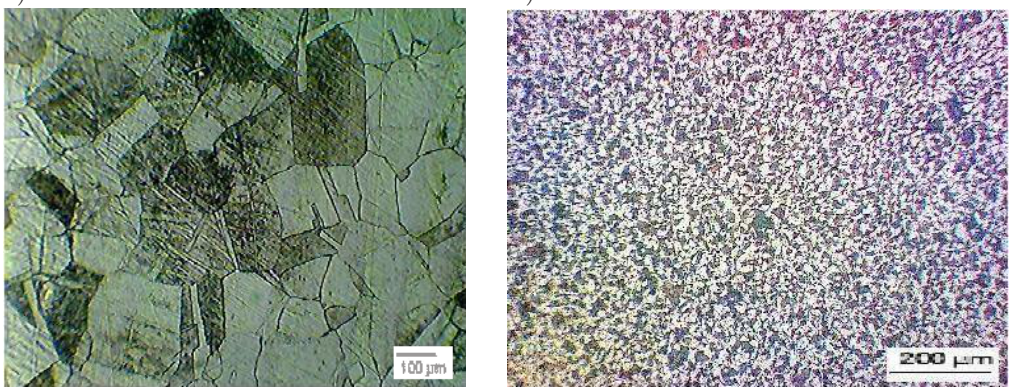

FIG. 2. a) Base metal X2CrNiMo17-12-2; b) base metal C40.

cles was observed both on the grain boundary and on the grains. In addition, marginal presence of some non-metallic inclusions was found. The wrought austenitic stainless steel displays a high percentage of elongation and marginal superplasticity at high temperature and therefore it can flow easily during welding.

The light microscopy photograph shown in Fig. 2b was taken with the use of 3% nital etch. The parent metal C40 has fine grained pearlite in a matrix of ferrite. The uniform grain suggests that the material was normalized.

3.2. Tensile strength

The highest value of the tensile strength 648.67 MPa was obtained from a sample welded with a friction pressure of 141 MPa, the upset pressure of 141 MPa, the speed of rotation of 1500 RPM, and a burn-off length of 3 mm; and the lowest value of 548.09 MPa was obtained from a sample welded with a friction pressure of 95 MPa, the upset pressure of 130 MPa, the speed of rotation of 1000 RPM, and a burn-off length of 3 mm. Both results are shown in Table 3. These results imply that the tensile strength was higher in the fraction welding process due to friction pressure. The heat which caused the grain to produce/release less carbon precipitation caused it to have no carbon line as well and imparted higher tensile strength to the weld. The materials were in a plastic state (without melting), which aided the grains at the weld boundary to undergo heavy pressure from both longitudinal and tangential directions, resulting in superfine size, and thus contributing to the tensile properties of the weld. The weld joints of these dissimilar metals and the fracture specimen are

Table 3. Taguchi's L9 orthogonal array & results of mechanical properties.

Experiment No	Friction pressure [MPa]	Upset pressure [MPa]	Speed of rotation [RPM]	Burn-off length [mm]	Tensile strength [MPa]	% of elongation
1	95	118	1000	3	548.09	3.40
2	95	130	1500	4	632.25	2.65
3	95	141	2000	5	570.67	6.10
4	118	130	1500	5	603.51	4.80
5	118	130	2000	3	578.88	4.10
6	118	141	1000	4	597.35	6.20
7	141	118	2000	4	630.19	5.50
8	141	130	1000	5	644.57	7.00
9	141	141	1500	3	648.67	7.04

a) b)

FIG. 3. a) Friction welded sample, b) fractured zone of weld joints.

shown in Fig. 3. The specimen illustrates the zone that is an interface between the parent metal zone of X2CrNiMo17-12-2 and C40. The fracture occurred at the side of parent metal X2CrNiMo17-12-2, what indicates good ductility of the weld joints.

3.3. Hardness

The values of hardness in different zones were taken as a survey and the readings are shown in Table 4. The conducted hardness survey showed that the hardness of the friction welded samples was quite high in the heat affected zones. In stainless steel, the presence of chromium transfers most of the heat and renders the grains coarser in the weld zone. The coarse grains make the joint

Table 4. Hardness values in different zones.

Sample No	EN 8		SS 316L	
	Parent	Heat affected zone	Parent	Heat affected zone
1	180.5, 188.5	259.2, 318.9	236.2, 242.2	477.8, 466.1
2	215.3, 213.7	300.9, 310.5	307.7, 305.5	393.0, 402.4
3	180.5, 188.5	291.8, 297.7	259.4, 262.2	301.9, 302.6
4	192.6, 188.7	308.3, 291.9	271.7, 266.3	359.4, 376.4
5	192.5, 182.0	262.3, 266.8	253.6, 276.6	438.2, 427.0
6	246.3, 249.3	297.5, 304.1	234.8, 240.9	304.6, 302.2
7	189.6, 184.3	306.5, 319.4	296.9, 116.6	401.1, 408.2
8	162.8, 170.2	358.7, 293.0	253.1, 264.7	648.6, 574.0
9	212.0, 215.0	327.5, 303.1	247.0, 257.6	332.6, 327.9

harder at the heat affected zone. Owing to the intense heat which is produced by friction pressure, a change from austenite to martensite occurs which in turn makes the friction welded sample to acquire high hardness. Molak *et al.* [9] investigated the measurement of mechanical properties in an X2CrNiMo17-12-2 stainless steel welded joint and found that the highest mechanical properties were better exhibited in the material taken from the heat affected zone than the weld material. It is generally assumed that the elevated chromium content of the weld metal along with the presence of niobium increases steel hardenability [12]. Kurt and Samur [6] reported that hardness was higher in the heat affected zone than in other regions.

3.4. Metallurgical studies

3.4.1. Macrostructure. Figure 4 shows the macrostructure of sample 9 which imparts the tensile strength of 648.07 MPa. The higher magnification image shows clearly the flow of grains from the X2CrNiMo17-12-2 material. The weldability of carbon steel is low probably due to the higher carbon equivalent of the material. The top portion of Fig. 4 depicts the stainless steel matrix and the bottom of the Fig. 4 shows the carbon steel. The interface is at the center with the bonding of the two metals. A good flow is observed due to better plasticity of the material. The carbon steel side shows the heat affected zone as dark due to the conversion of the martensite caused by the thermal effect. This martensitic transformation causes the weld joint to acquire high tensile strength.

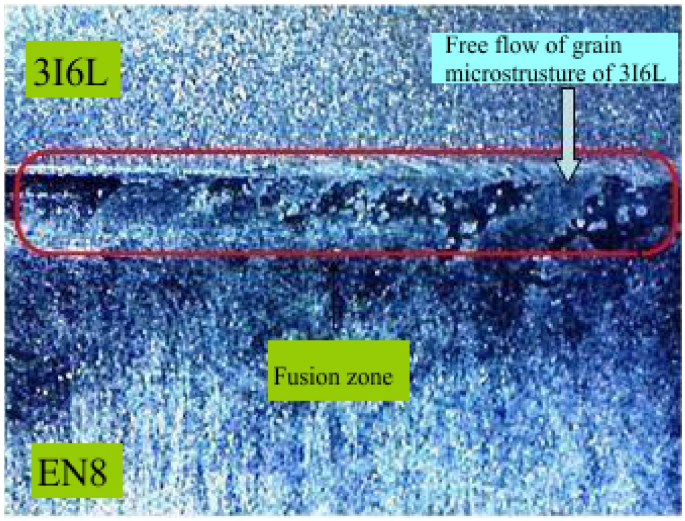

Fig. 4. Macrostructure of the weld joint (for sample 9).

3.4.2. Microstructure of weld joints. Figures 5a and 5b represent the interface zone of the samples 1 and 9 and Figs. 5c and 5d represent the weld zone of sample 1 and 9 respectively. The austenite grain flows towards the C40 side due to diffusion. Owing to its thermal effects the elements are transformed in to martensite and there is a flow line in X2CrNiMo17-12-2 region. The heat affected region is wider in sample 9 than that in sample 1. The HAZ (heat affected zone) plays a vital role in enhancing mechanical properties.

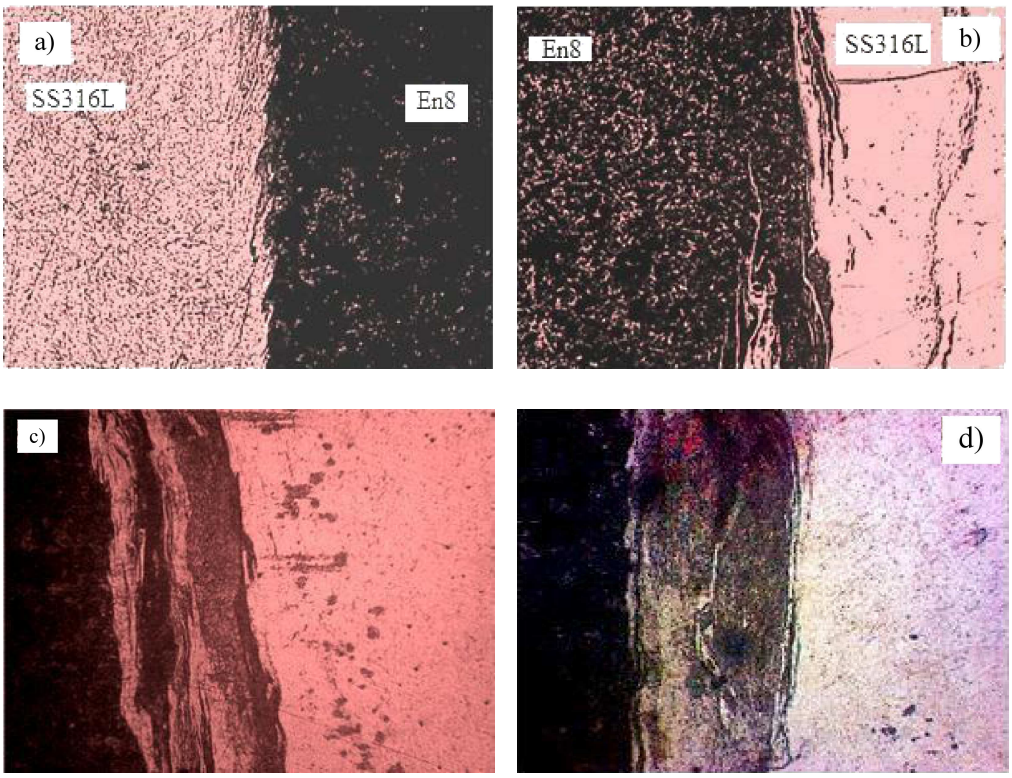

FIG. 5. Interface zone for sample 1 (a), for sample 9 (b), weld zone for sample 1 (c) and for sample 9 (d).

3.4.3. SEM analysis. Scanning electron microscopy (SEM) was used to describe the outcome of the fracture process and the modes of failure [3]. Specimens that failed in tensile tests were used in the SEM study. Figure 6 shows the image of the fractured tensile specimen, fractured at the X2CrNiMo17-12-2 region. The fractured neck of the specimen shows good yielding with the formation of conical shape. The SEM image shows a typical ductile fractured surface. The surface at 500X shows fine dimples with uniform distribution throughout the

a)

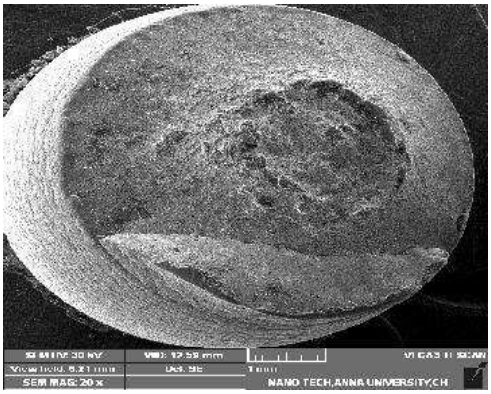

b)

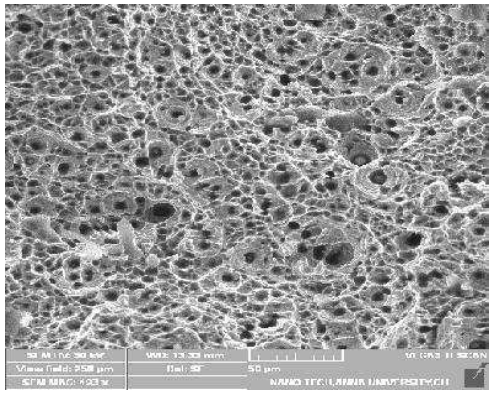

c)

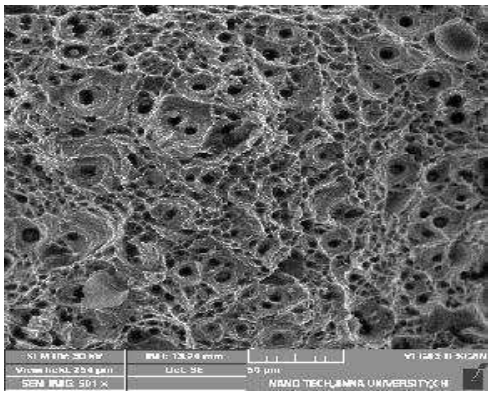

FIG. 6. a) Formation of conical shape, b) ductile fracture zone, c) elongated dimples on X2CrNiMo17-12-2side.

field. This suggests the homogeneity of the matrix and higher percentage elongation of the specimen. Some of the un-definable spots (inclusions) observed in the photomicrograph are referred to as voids. These voids are obtained after necking. They indicate the plastic deformation which occurs at the yield point. Elongated dimples are formed by the fracture. They are better resolved showing the uniformity at the fracture surface. More uniform dimple appearance indicates that the fracture is ductile in nature.

3.4.4. XRD analysis. XRD analysis of the prepared sample was performed with a Goniometer under 30 kV/100 mA with X-ray scanning mode being continuous with filter Cu K-beta with the scan range of 20 to 80 degrees with

a step of 0.02 degree. Peaks at 2-theta values of 43.43, 44.53, 50.65, 74, and 50 degrees corresponding to (1,1,1), (1,0,0), (2,0,0), and (2,2,0) planes of iron (Fe), chromium (Cr) and carbon (C) were observed with the JCPDS card of file Nos. 9013488, 9008467, and 9012592 respectively. This XRD confirmed that the resulting chromium particles were uniformly spread in the weld zone to improve corrosion resistance of the weld joint which is shown in Fig. 7.

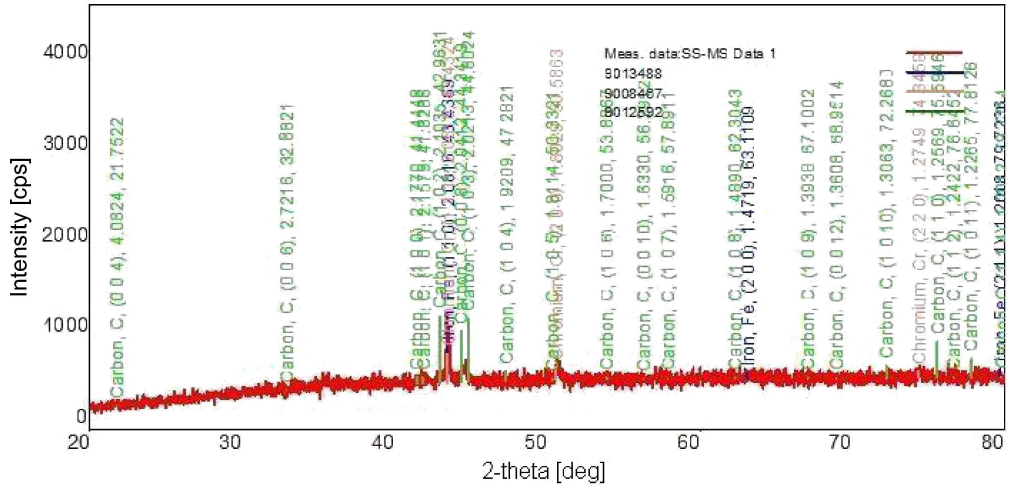

FIG. 7. XRD for high tensile strength.

3.4.5. Corrosion studies. Potentiodynamic polarization and its micro structural studies were carried out for the low and high tensile stress samples in 3.5% NaCl solution at ambient temperature. Table 5 depicts the studies carried out on samples which had low and high tensile strengths (1, 9) even though there were similarities in the pattern; the rest potential was high for sample 9. This shows that the bonding of the two materials with the constituents of X2CrNiMo17-12-2 is higher. Hence the resistance of the friction zone shows an increased potential

Table 5. Corrosion results for weld joints subjected with 3.5% NaCl solution.

Sample I.D.	I_{corr} (corrosion current) [mA/cm^2]	Corrosion rate [mm/year]	Corrosion rate [mills/year]	Area of the sample [cm^2]	Rest potential [mV]
S-1	1.2605	14.61	575.2	1	−521.2
S-9	0.767	8.89	350.27	1	−554.8

to overcome ionization. This has a direct impact on tensile properties. It means that the diffusion of the stainless steel constituents towards the Bi-metallic zone is increased resulting in the enhanced tensile strength. Friction weld process showed that the diffusion of the stainless steel constituents diluted towards the low carbon steel at the friction zone. From the macrostructure and microstructure examinations it was observed that the plastic flow of the stainless steel was higher for sample 9.

The potentiodynamic polarization studies showed that the rest potential for sample 9 (−554.8 mV) behaved better towards sample 1 (−421.2 mV). In addition, the tensile values were higher for sample 9. This might be due to the flow of constituents like chromium, nickel and molybdenum that could significantly affect the corrosion resistance of stainless steel [7, 14] which was evident for sample 9.

4. Conclusion

- The joining of X2CrNiMo17-12-2 with C40 medium carbon steel using CDDFW method was conducted and the mechanical, metallurgical and corrosion properties were investigated.
- Maximum tensile strength of 648 MPa was obtained by varying the process parameters such friction pressure, upset pressure, speed and burn-off length. The welded samples were broken at the X2CrNiMo17-12-2 side due to its ductility.
- High hardness was obtained in the heat affected zone when compared with base metal and the weld zone.
- The macrostructural study showed that the flow of austenitic grains was transferred from the X2CrNiMo17-12-2 region to C40 region.
- The microstructural study showed that some elements got transformed into the marten site phase in the C40 region due to the thermal effects and the flow line of elements in X2CrNiMo17-12-2 was observed. The fractured zone showed the elongated dimples in homogeneous matrix revealing the ductile fracture that had occurred in the fractured zone.
- The peak value obtained from the XRD analysis confirmed that the weld zone had chromium particles that were consistently spread to improve the corrosion resistance properties.
- Corrosion studies were conducted on high as well as low tensile strength specimens. They showed that corrosion resistance was higher in specimen 9 due to the presence of chromium with the obtained corrosion rate of 8.98 mm/year which had high tensile strength.

Acknowledgment

The authors would like to express their gratitude to Sri Chandrasekharendra Saraswathi Viswa Maha Vidyalaya, Kanchipuram and St. Joseph's College of Engineering, Mr. R. Rangan Senior technician IIT-M, Chennai.

References

1. Amudarasan N.V., Palanikumar K., Shanmugam K., *Impact behaviour and micro structural analysis of AISI 316L stainless steel weldments*, International Journal of Application or Innovation in Engineering & Management, **2**(6): 269–272, 2013.
2. Ananthapadmanaban D., SeshagiriRaov V., Vijayan D., Muthu Vaidyanathan R., Prasad Rao K., *A review of friction welding processes in similar and dissimilar materials*, International Journal of Design and Manufacturing Technologies, **3**(2): 68–72, 2009.
3. Cui Y., Lundin C.D., Hariharan V., *Mechanical behaviour of austenitic stainless steel weld metals with microfissures*, Journal of Materials Processing Technology, **171**(1): 150–155, 2006.
4. Datta S., Bandyopadhyay A., Pal P.K., *Grey-based Taguchi method for optimization of bead geometry in submerged arc bead-on-plate welding*, International Journal of Advanced Manufacturing Technology, **39**(11): 1136–1143, 2008.
5. Dhananjayulu A., Ratnesh Kumar R.S., Dwivedi D.K., Mehta N.K., *Effects of friction stir welding on microstructural and mechanical properties of copper alloy*, International Journal of Mechanical, Aerospace, Industrial, Mechatronic and Manufacturing Engineering, **5**(2): 336–344, 2011.
6. Kurt H.I., Samur R., *Study on microstructure, tensile test and hardness of 316 stainless steel jointed by TIG welding*, International Journal of Advances in Engineering, Science and Technology, **3**(1): 1–6, 2013.
7. Kožuh S., Gojić M., Kraljić Roković M., *The effect of PWHT on electrochemical behaviour of AISI 316L weld metal*, Chemical and Biochemical Engineering Quarterly, **22**(4): 421–431, 2008.
8. Lienert T.J., Stellwag W.L., Grimmett B.B., Warke R.W., *Friction stir welding studies on mild steel.* Welding Journal, Research Supplement, **1**: 1–9, 2003.
9. Molak R.M., Paradowski K., Ciupiński Ł., Pakiela Z., Brynk T., Kurzydłowski K.J., *Measurement of mechanical properties in a 316L stainless steel welded joint*, International Journal of Pressure Vessels and Piping, **86**(1): 43–47, 2009.
10. Reynolds A.P., Tang W., Gnaupel-Herold T., Prask H., *Structure, properties, and residual stress of 304L stainless steel friction stir welds*, Scripta Materialia, **48**(9): 1289–1294, 2003.
11. Satyanarayana V.V., Madhusudhan Reddy G., Mohandas T., *Dissimilar metal friction welding of austenitic-ferritic stainless steel*, Journal of Material Processing Technology, **160**(2): 128–137, 2005.
12. Sourmail T., *Precipitation in creep resistant austenitic stainless steels*, Materials Science and Technology, **17**(1): 1–14, 2001.

13. Kožuh S., Gojić M., Kosec L., *The effect of annealing on properties of AISI 316L base and weld metals*, RMZ – Materials and Geoenvironment, **54**(3): 331–344, 2007.

14. Liptáková T., Alaskari A., Halamová M., *Surface treatment of the AISI 316L after welding and study of corrosion*, Periodica Polytechnica, Transporation Engineering, **41**(2): 143–147, 2013.

15. Vill V.I., *Friction welding of metals*, New York American Welding Society, New York, 1962.

Received September 7, 2015; accepted version February 20, 2016.